JOURNAL OF MATERIALS SCIENCE **36** (2001) 3511 – 3518

Thermal conductivity and phase evolution of plasma-sprayed multilayer coatings

Y. JENNIFER SU
Department of Materials Science and Engineering, Northwestern University, Evanston, IL, USA

HSIN WANG, WALLY D. PORTER
High Temperature Materials Laboratory, Oak Ridge National Laboratory, Oak Ridge, TN, USA

A. R. DE ARELLANO LOPEZ
Departamento de Fisica de la Materia Condensada, Universidad de Sevilla, Seville, Spain

K. T. FABER
Department of Materials Science and Engineering, Northwestern University, Evanston, IL, USA
E-mail: k-faber@northwestern.edu

Multilayer coatings were prepared using small-particle plasma spray to investigate the effect of interfaces on thermal conductivity and phase stability. Monolithic and multilayer alumina and yttria partially-stabilized zirconia coatings, with 0, 3, 20, and 40 interfaces in 200–380 μm thick coatings were studied. Thermal conductivity was determined for the temperature range 25 °C to 1200 °C using the laser flash method and differential scanning calorimetry. Thermal conductivity of the multilayer coatings was accurately modeled by a series heat transfer equation, indicating that interfacial resistance plays a negligible role in heat transfer in the direction perpendicular to the coating plane. Powder X-ray diffraction results indicate that identical phase transitions occur in all the coatings. Independent of coating microstructure (i.e. layer thickness), as-sprayed γ-Al_2O_3 transforms to α-Al_2O_3 after 100 hours at 1200°C; as-sprayed metastable t′–ZrO_2 converts to a mixture of t–ZrO_2 and c–ZrO_2 after 100 hours at 1300 °C. Thus, the results indicate that the interfaces do not aid in stabilizing the as-sprayed phases after prolonged severe heat treatments.

1. Introduction

Thermal barrier coatings (TBC's) are often used to improve the efficiency of gas turbine engines by allowing increased operating temperatures and/or reduced cooling rates. They typically consist of two layers: an intermediate metallic bond coat and a ceramic top coat. The bond coat, typically an MCrAlY (where M = Co, Fe, or Ni), improves coating adherence by reducing the coefficient of thermal expansion (CTE) mismatch between the metal substrate and the ceramic top coat [1] and by allowing formation of an adherent Al_2O_3 scale. The primary purpose of the top coat is to provide thermal resistance in the direction perpendicular to the substrate surface. Partially stabilized 6–8 wt.% yttria-stabilized zirconia (YSZ) is the most commonly used top coat material. It possesses the desired properties of a relatively low thermal conductivity and high CTE. Nevertheless, to further increase coating lifetime and engine performance, coatings with improved performance characteristics are continually being sought.

One approach to altering the properties of TBC's is to incorporate multiple phases. Functionally graded materials (FGM) have been proposed for their potential to reduce residual stress development and improve oxidation protection [2–4]. To reduce the thermal conductivity, particulate composite [5] or multilayer [6–9] architectures can be used. In both systems, heat resistance can be increased by adding a lower thermal conductivity second phase. However, the multilayer structures may also aid in phase stability [10] at high temperatures. As in the case of zirconia, as-sprayed phases (e.g. t′–ZrO_2) can have a lower thermal conductivity than those formed after extended high temperature exposure (e.g. m–ZrO_2) [11]. Thus, phase stability at high temperatures is also an important issue.

Assuming a slab geometry and negligible interfacial resistance, the lower bound on the conductivity of a multilayer material, k_{ML}, can be calculated using a series heat-transfer model [12]:

$$k_{ML} = (k_1 k_2)/(v_1 k_2 + v_2 k_1) \quad (1)$$

where "v" is the volume fraction and the subscripts "1" and "2" refer to the individual materials (Fig. 1). If

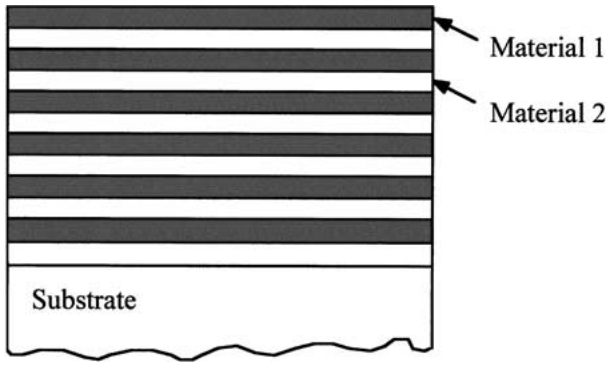

Figure 1 Schematic drawing of a multilayer material with alternating slabs of material 1 and 2.

the interfaces play a role in reducing heat conduction, then the experimentally determined thermal conductivity values will be lower than those calculated using Equation 1.

Recently, An *et al*. studied the influence of layering Al_2O_3 and YSZ on the thermal conductivity of electron beam physical-vapor deposited (EB-PVD) coatings [6]. Based on crystallographic texture measurements via pole figures, it was suggested that epitaxial growth between the layers reduced any potential interfacial thermal resistance. To further explore the effect of imperfect interfaces, they later extended this work to plasma-sprayed multilayer coatings of up to 16 alternating layers of the two materials [7]. We describe here the development of multilayer coatings via the small-particle plasma spray (SPPS) technique that affords finer layers than conventional plasma spray. We probe the influence of up to 40 layers on the thermal conductivity and phase evolution of alumina Al_2O_3/zirconia (YSZ) multilayer, as well as monolithic, coatings at temperatures of interest for thermal barriers.

2. Experimental materials and methods

2.1. Coating materials and plasma spray processing

Samples were produced using small-particle plasma spray (SPPS), an air plasma spray system which incorporates a beveled powder injection tip [13]. A Plasma-Tecknik F4 gun with a 6 mm nozzle was used to fabricate all samples. The average particle size of the starting Al_2O_3 (Praxair Al-1110-HP) and YSZ (H. C. Stark Amperit 825.0) powders were 9 μm and 12 μm, respectively. The specific spray parameters used for each material are listed in Table I.

TABLE I Spray parameters for alumina and yttria-stabilized zirconia powders

Spray parameter	Al_2O_3	YSZ
Power (kW)	45	35
Argon primary gas flow (slm)	41.7	32.0
Hydrogen secondary gas flow (slm)	8.3	8.0
Injector angle (degrees)	30	40
Injector radial offset (mm)	9	11
Spray distance (cm)	6	6
Argon carrier gas flow (slm)	5	5

Two separate powder feeders and injectors were used in an alternating fashion to deposit multilayer coatings on 220 grit-blasted aluminum-coated 1018 mild steel substrates. The number of gun passes across the substrate was varied to control the layer thickness. In total, multilayer coatings 200–380 μm thick, consisting of 3, 20, and 40 interfaces, were produced. Two monolithic coatings, one containing pure YSZ and the other pure Al_2O_3, were also fabricated. Samples were soaked in a dilute solution of hydrochloric acid to preferentially etch the aluminum and create free-standing coatings for testing.

2.2. Thermal property measurements

Thermal diffusivity measurements of free-standing coatings were made using the laser flash technique [14]. All measurements were conducted at Oak Ridge National Laboratory in the High Temperature Materials Laboratory [15]. Samples were disk-shaped ($\sim$12.5 mm in diameter) and varied from 250 μm to 380 μm in thickness. Coating thickness was measured using a micrometer. A Nd : Glass laser was used to produce a heat pulse aimed at the front face of the sample. From room temperature to 500 °C an aluminum furnace and InSb detector were used to monitor the temperature of the sample's back face. At higher temperatures (600–1200 °C) a graphite furnace and Si detector were used. Each sample's front and back surface was coated with graphite to make the material opaque. All samples were tested in an inert argon atmosphere. Time versus temperature curves were recorded using 16 KHz high-speed data acquisition. Thermal diffusivity was calculated following ASTM standard E1461 [16]. The software performed pulse-width correction to the raw data. The reported thermal diffusivity data were obtained using the Clark and Taylor [17] method, which accounts for radiation heat losses and derives a corrected half-rise time. The thermal diffusivity, α, was calculated from the coating thickness, l, and the corrected half rise time, $t_{1/2}$:

$$\alpha = \frac{Al^2}{t_{1/2}} \tag{2}$$

where A is a dimensionless parameter. Six samples were tested concurrently and three measurements were taken and averaged for each specimen at each temperature. One replicate was run for each sample.

Specific heat was measured using a differential scanning calorimeter (Stanton Redcroft DSC1500) comparative method with a sapphire standard. Sample disks 4 mm in diameter were stacked to obtain a weight of approximately 90 mg. The heat flow was measured from 25 °C to 1000 °C with a 20 °C/min ramp up rate. All samples were heat treated for 1 hour at 1000 °C in air prior to the measurement because some as-sprayed samples produced unstable exothermic reactions around 900 °C. A best fit line of specific heat vs. temperature data was extrapolated to obtain values between 1100 °C and 1200 °C.

The Archimedes' water immersion technique was used to measure coating density and total porosity.

Three measurements were taken and averaged for each coating. Thermal conductivity, k_T, was then calculated using the following equation:

$$k_T = \alpha(T)C_p(T)\rho \quad (3)$$

where T is temperature, α is thermal diffusivity, C_p is specific heat, and ρ is density. Based on the error associated with the three individual factors, the total error associated with the full set of measurements was estimated to be approximately 6%.

2.3. Phase stability studies

Combustion exhaust gas environments in commercial gas turbine engines can reach temperatures of 1300 °C or higher [18]. To study the behavior near service temperatures, samples were heated for 100 hours in air at 1000 °C, 1200 °C, and 1300 °C. X-ray powder diffraction was performed on as-sprayed and heat-treated coatings using a Rigaku Giegerflex Diffractometer and Cu K_α radiation. In some cases, an internal aluminum standard was used to determine any diffraction angle offset associated with the experimental set-up. Following the work of Muraleedharan [19], the 72–76° 2θ region was analyzed in greater detail to identify the zirconia phases.

3. Results and discussion

3.1. Coating microstructure

SEM images of the various coatings are shown in Fig. 2. Image analysis was used to determine the volume fraction of each phase in the multilayer coatings (Table II). There is excellent interfacial contact between the Al_2O_3 and YSZ layers. A TEM micrograph of the interface shows the lack of interlayer porosity and the high degree of bonding (Fig. 3).

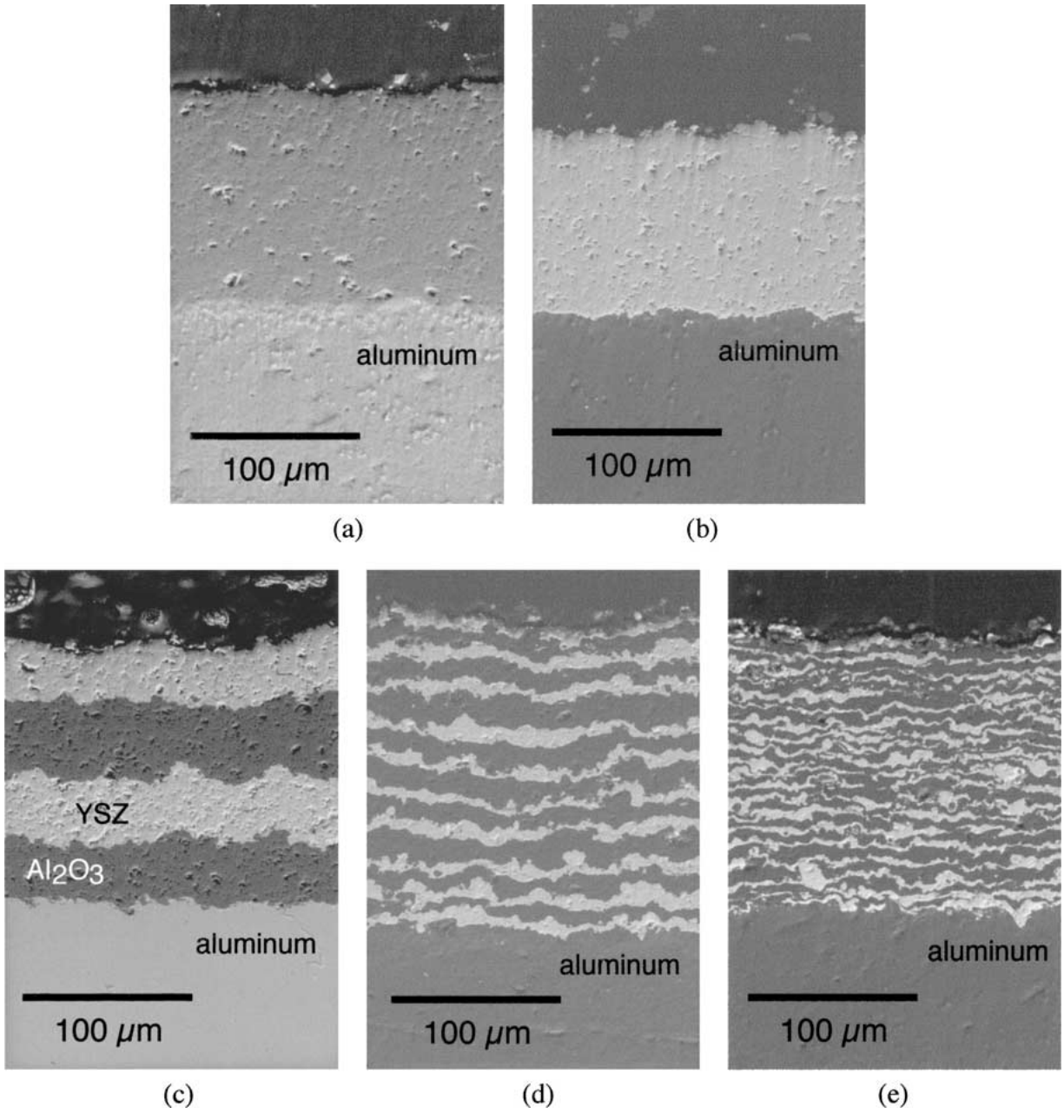

Figure 2 Cross-sectional SEM micrographs of (a) pure alumina, (b) pure YSZ, (c) AY3, (d) AY20, and (e) AY40 multilayer coatings.

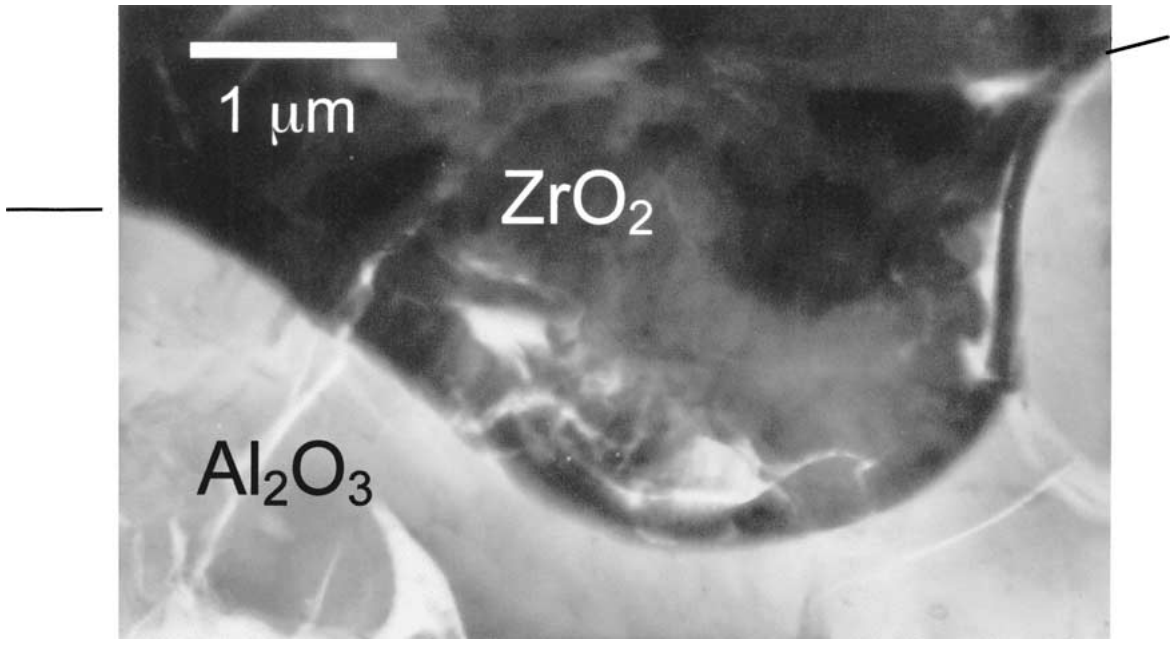

Figure 3 TEM image of an alumina/zirconia interface which reveals the high degree of interfacial contact. The black lines denote the interface between the alumina and zirconia.

TABLE II Specifications for monolithic and multilayer coatings

Sample	Number of interfaces	Volume percent of alumina	Volume percent of zirconia	Density (g/cm^3)	Theoretical density (g/cm^3)	Total porosity (%)
AY40	40	60	40	3.86	4.77	19.0
AY20	20	50	50	—	—	—
AY3	3	50	50	4.15	4.99	16.9
Monolithic YSZ	—	0	100	5.33	6.08	12.3
Monolithic Al_2O_3	—	100	0	3.36	3.90	14.0

Delamination between the alumina and zirconia was not observed, even after long term high temperature exposure (Fig. 4). Such sustained bonding and layer integrity was not reported in previous studies [7].

3.2. Thermal conductivity of monolithic coatings

Typically, the thermal conductivity of plasma-sprayed coatings is significantly lower than that of the corresponding bulk material. This is a well-documented phenomenon which is attributed to increased thermal resistance due to interlamellae boundaries [20], porosity [11], and microcracks parallel to the coating plane [11, 21]. Fig. 5a shows the thermal conductivity results for the monolithic coatings, as well as for the dense bulk materials. The bulk alumina data [22] are for α–Al_2O_3 because data for γ–Al_2O_3 were not available. As expected, the thermal conductivity of the alumina coating is significantly lower than that for dense alumina. The initially low room temperature thermal conductivity of both coatings is an artifact due to the high sensitivity of thermal diffusivity measurements on the laser power level [23].

Conversely, the monolithic YSZ coating actually exhibits a relatively high thermal conductivity for a plasma-sprayed material. In fact, the values match well with those of the bulk material as measured by Hasselman [24]. The data from Hasselman were obtained for bulk t–ZrO_2. Since specific heat is a material property, independent of microstructure, the unexpected conductivity values of the coating can be attributed to high density and/or high thermal diffusivity values. Upon comparison with published bulk thermal diffusivity values [25], it is clear that the YSZ coating does possess a relatively high thermal diffusivity (Fig. 5b). The measured values for the coating are comparable to the bulk diffusivity values. SPPS YSZ coatings may have higher densities than conventionally air plasma-sprayed YSZ. However, due to the use of and relatively large uncertainties of many density measurement techniques (immersion, image analysis, MIP), it is difficult to compare values across studies.

The reason behind these unexpectedly high diffusivity values is not yet clear. It has been observed that the selected spray parameters (e.g. starting powder specifications, power level, and gases) can have a significant effect on the thermal diffusivity of plasma-sprayed coatings [26, 27]. The effect has been attributed to differences in coating microstructure that arise under various spray conditions. Lamellae thickness, degree of intersplat contact [28], and extent of microcracking [29] are known to greatly affect the thermal properties of plasma-sprayed coatings. Therefore, it is speculated that the chosen spraying conditions resulted in microstructural features that decreased the thermal resistance beyond what is typically observed for as-sprayed coatings.

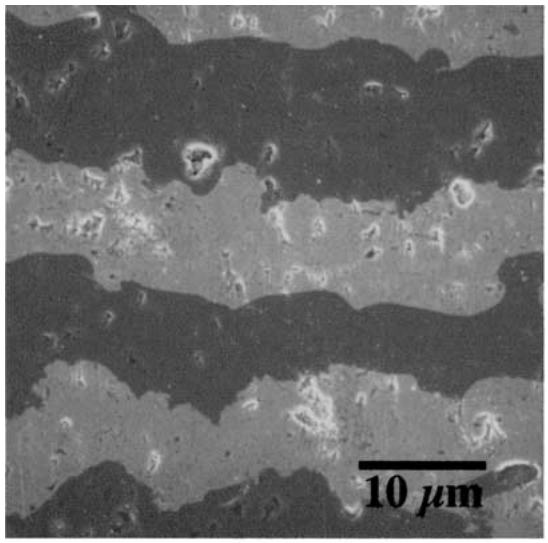

(a)

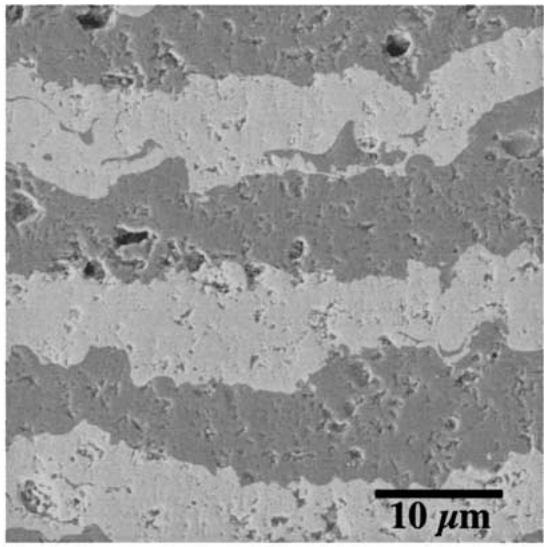

(b)

Figure 4 SEM micrographs reveal the high degree of interfacial contact between layers of alumina (darker) and zirconia (lighter) in the (a) as-sprayed and (b) heat-treated [1000 °C/100 h] coating.

3.3. Thermal conductivity of layered coatings

The thermal conductivity measurements for the AY40 and AY3 multilayer coatings are shown in Fig. 6. The values predicted by Equation 1 are also plotted in Fig. 6. The slight decrease observed between 500–600 °C is an artifact attributed to switching furnaces during the diffusivity tests. The experimental results agree well with the series heat-transfer model, indicating a lack of interfacial thermal resistance in both coatings. This is not surprising due to the high degree of bonding and lack of additional porosity at the alumina/zirconia interfaces (Fig. 3).

The discrepancy between the AY3 sample data and the model can be attributed to surface roughness effects and variability in layer thickness. The surface roughness inherent to the top surface of plasma-sprayed coatings can introduce error in coating thickness measurements. Relatively small errors in coating thickness measurements can cause a noticeable shift in the thermal conductivity [7, 30]. A 4% error in coating thickness can produce a 10% change in the thermal conductivity [30]. The surface roughness characteristic of plasma-sprayed coatings could introduce such an error in thickness. To obtain more accurate thickness measurements, the coatings should be polished plane parallel after removal from the substrate. Another potential source of error is the variability in layer thickness. The SEM micrographs clearly reveal the variation that can occur across a relatively short distance (Fig. 2c–d). Due to this variability in layer thickness, different localized regions will have slightly different percentages of each phase. This will introduce error into the volume fraction measurements conducted by image analysis.

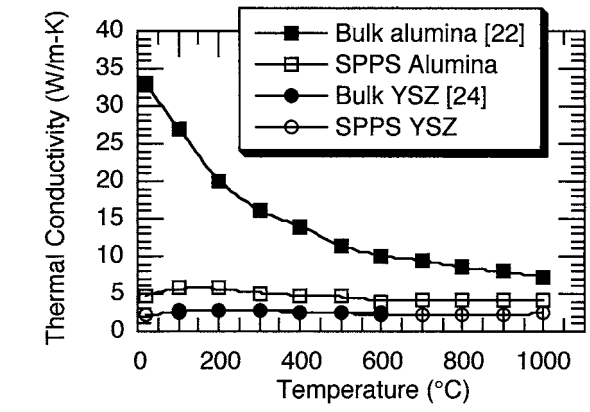

(a)

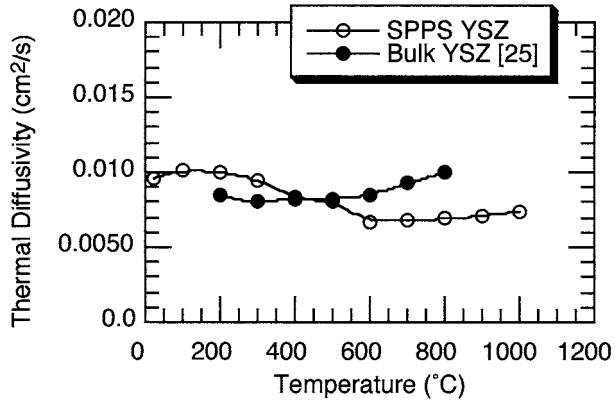

(b)

Figure 5 (a) Thermal conductivity of pure YSZ and pure Al_2O_3 coatings compared to bulk values (b) Thermal diffusivity of YSZ coating compared to bulk value.

The results in this investigation are consistent with recent work on plasma-sprayed [7] and EB-PVD [6] multilayer coatings. These three studies collectively demonstrate that the existence of up to 50 interfaces do not affect heat transfer in the alumina/zirconia system. In all cases, a series heat transfer equation accurately models the thermal conductivity in the multiphase coating.

3.4. Phase stability at high temperature

As-sprayed 7 wt% YSZ is typically present as metastable t′–ZrO_2. Coating durability has been directly linked to the percentage of this phase [31]. However, t′–ZrO_2 is diffusionally unstable at high temperatures and will revert to equilibrium t–ZrO_2 [31]. Upon cooling, t–ZrO_2 can further transform to the monoclinic phase, resulting in a 4.5% volume expansion.

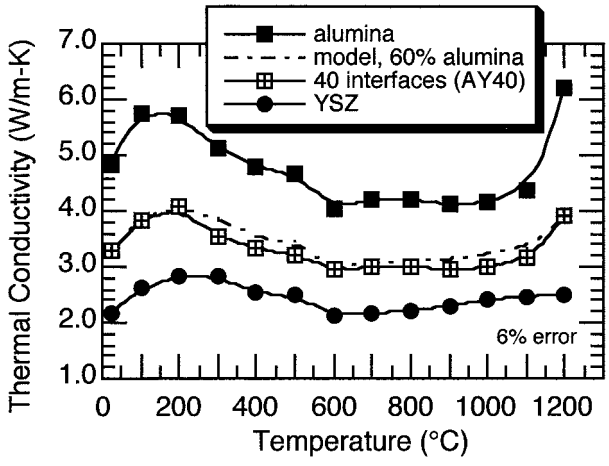

(a)

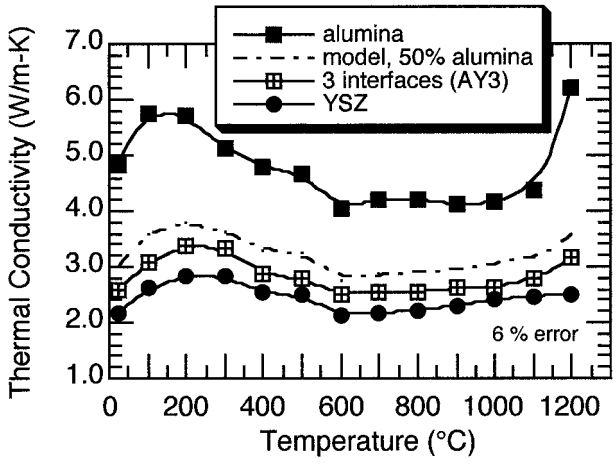

(b)

Figure 6 Thermal conductivity of monolithic coatings and series heat transfer model prediction plotted with (a) AY40 (b) AY3 sample data.

In a similar manner, as-sprayed γ–Al_2O_3 is unstable at high temperatures. The transformation of γ–Al_2O_3 to α–Al_2O_3 at high temperatures results in an 11% volume reduction.

Conceptually, the alumina/zirconia interfaces could serve as physical barriers that hinder these phase transformations. It was speculated that alumina/zirconia interfaces in the layered coatings would limit diffusion and inhibit phase transformations that would otherwise occur in pure coatings. Since alumina and zirconia are immiscible, these multilayer systems are ideal for stability studies. A similar approach towards phase stability has been taken by Andritschky *et al*. using ceramic PVD coatings [10].

3.4.1. Alumina

X-ray diffraction results for the monolithic alumina coating are presented in Fig. 7a. The starting powder is present as α–Al_2O_3. Although α–Al_2O_3 is the stable equilibrium phase, metastable γ–Al_2O_3 forms during plasma-spraying due to its lower critical free energy for nucleation and the rapid quench rate during splat formation [32]. Both γ and α phases are observed in the monolithic as-sprayed coating. Based on calculations by McPherson which incorporate particle size and time-temperature behavior in the flame [32] the formation of γ–Al_2O_3 is expected for this system. Additionally,

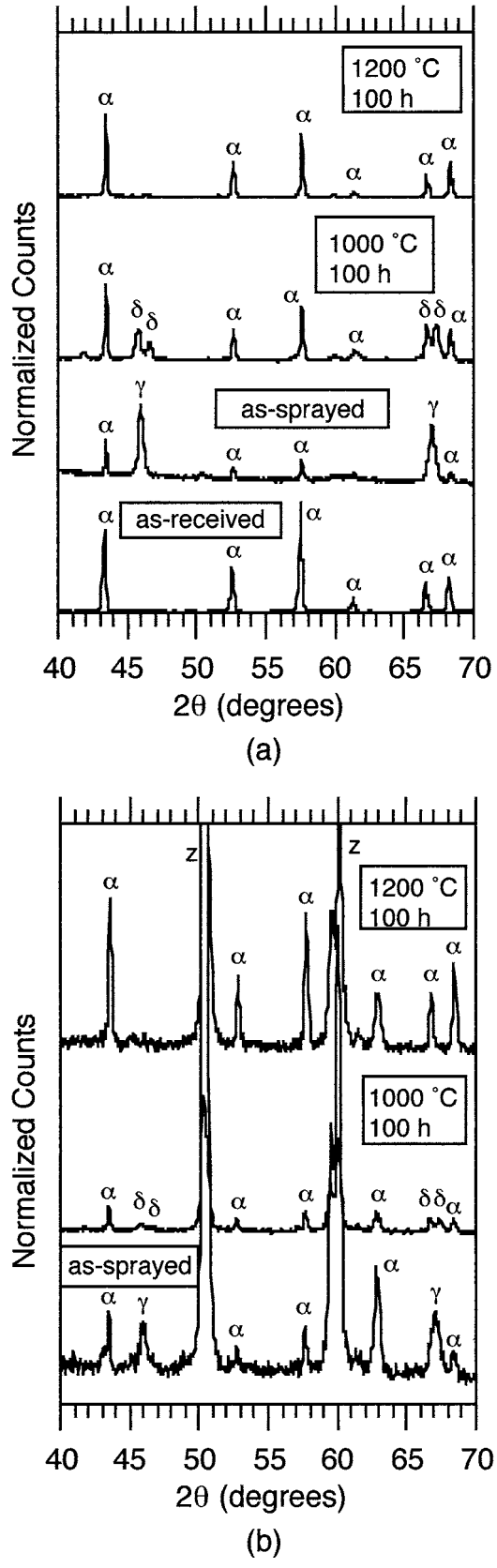

(a)

(b)

Figure 7 X-ray diffraction pattern of alumina in the as-sprayed and heat treated conditions: (a) monolithic and (b) AY40 multilayer coatings. (α, γ, and δ = alumina, z = zirconia).

there is a significant number of unmelted α–Al_2O_3 particles in the microstructure [33]. Upon heat treatment at 1000 °C for 100 hours, the γ to δ phase transition is observed (Fig. 7a). After exposure at 1200 °C for 100 hours, the complete transformation to α–Al_2O_3 occurred. The γ to δ to α phase transformation has also

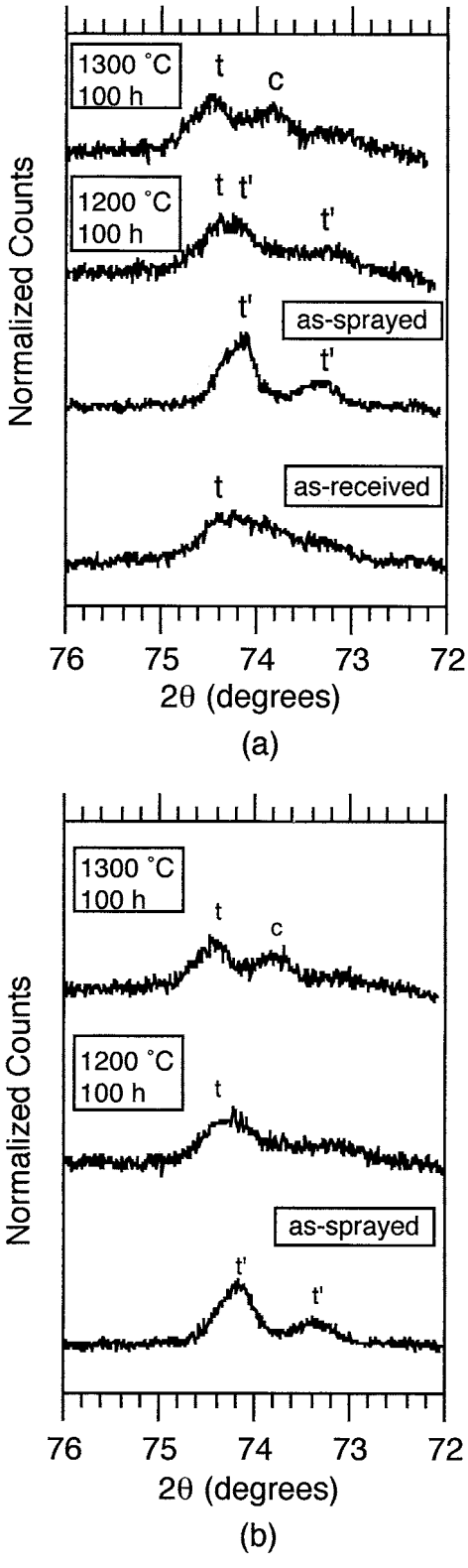

Figure 8 X-ray diffraction patterns of zirconia coatings in the as-sprayed and heat treated conditions for a (a) monolithic and (b) AY40 multilayer coating.

been observed in vapor-deposited amorphous alumina [34]. The γ-to-α phase transition observed in the monolithic alumina was observed in all of the layered samples (Fig. 7b). The interlayer interfaces do not appear to hinder the equilibrium transformation.

3.4.2. Zirconia

The results for zirconia-containing samples are shown in Fig. 8. The starting powder is present in the equilibrium t phase. As expected, as-sprayed YSZ is present as metastable t′–ZrO_2. Upon heat treatment the monolithic (Fig. 8a) and layered (Fig. 8b) samples all experience similar phase transformations. After 100 hours at 1200 °C, the t′–ZrO_2 begins to break down into a mixture of t–ZrO_2 and c–ZrO_2; however, a residual amount of t′–ZrO_2 is still present. Upon heating to 1300 °C for 100 hours, the t′–ZrO_2 fully transforms to t–ZrO_2 and c–ZrO_2. Monoclinic zirconia was not observed in any of the samples. The multilayer sample behaved similarly to the monolithic YSZ coating. Again, the interfaces do not noticeably affect nominal phase transitions.

These finding are consistent with Andritschky's work on PVD multilayer coatings [10]. They reported that coatings containing 1 nm thick alumina and 5 nm thick zirconia layers did not possess additional phase stabilization, despite a limited 5 nm grain size observed in the as-deposited coating. However, their results were partially due to physical layer instability and discontinuity after extended exposure to high temperatures. As mentioned above, the plasma-sprayed coatings in this study maintained excellent physical integrity after heating (Fig. 4).

4. Conclusions

Monolithic and multilayer plasma-sprayed coatings of up to 40 layers were fabricated and the thermal conductivity and phase stability were characterized. A series heat transfer equation adequately describes the thermal conductivity of plasma-sprayed multilayer coatings, as measured by the laser flash method and differential scanning calorimetry. The results suggest a negligible amount of interfacial heat resistance is present. Secondly, X-ray diffraction reveals that high temperature phase transformations which occur in monolithic alumina and yttria-stabilized zirconia coatings also occur in multilayer coatings. As-sprayed γ–Al_2O_3 fully transforms to α–Al_2O_3 after 100 hours at 1200 °C. As-sprayed YSZ evolves from t′–ZrO_2 to a t–ZrO_2 and c–ZrO_2 mixture after 100 hours at 1300 °C.

Acknowledgments

The authors wish to thank Rick Marzec of the Advanced Coatings Technology Group at Northwestern University for his assistance in fabricating the coatings. This work was supported by the U.S. Department of Energy, Federal Energy Technology Center, Cooperative Agreement No. DE-FC21-92MC29061, under subcontract 96-01-SR047. The thermal conductivity testing was supported by U.S. DOE, Assistant Secretary for Energy Efficiency and Renewable Energy, Office of Transportation Technologies, as part of the HTML User Program under contract DE-AC05-96OR22464, managed by Lockheed Martin Energy Research Corporation.

References

1. W. J. BRINDLEY and R. A. MILLER, *Advanced Materials and Processes* **8** (1989) 29.

2. M. I. MENDELSON, T. N. MCKECHNIE and L. B. SPIEGEL, *Ceramic Engineering and Science Proceedings* **15**(4) (1994) 555.
3. W. Y. LEE, D. P. STINTON, C. C. BERNDT, F. ERDOGAN, Y.-D. LEE and Z. MUTASIM, *J. Amer. Ceram. Soc.* **79**(12) (1996) 3003.
4. S. SAMPATH, H. HERMAN, N. SHIMODA and T. SAITO, *MRS Bulletin* **20** (1995) 27.
5. R. W. TRICE, Y. J. SU, K. T. FABER, H. WANG and W. PORTER, *Mat. Sci. and Engr. A* **272** (1999) 284.
6. K. AN, K. S. RAVICHANDRAN, R. E. DUTTON and S. L. SEMIATIN, *J. Amer. Ceram. Soc.* **82**(2) (1999) 399.
7. K. S. RAVICHANDRAN and K. AN, *ibid.* **82**(3) (1999) 673.
8. A. M. RITTER, J. R. RAIRDEN and R. L. MEHAN, *Mat. Res. Soc. Symp. Proc.* **190** (1991) 17.
9. M. C. RADHAKRISHNA, H. J. DOERR, C. V. DISHIPANDEY and R. F. BUNSHAH, *Surface and Coatings Technology* **36** (1988) 143.
10. M. ANDRITSCHKY, I. CUNHA and P. ALPUIM, *ibid.* **94/95** (1–3) (1997) 144.
11. S. RAGAHAVAN, H. WANG, R. DINWIDDIE, W. PORTER and M. J. MAYO, *Scripta Mater.* **39**(8) (1998) 1119.
12. W. D. KINGERY, "Introduction to Ceramics" (John Wiley and Sons, New York, 1976) p. 636.
13. T. F. BERNECKI and D. R. MARRON, Small Particle Plasma Spray Apparatus, Methods, and Coated Article, 1998 and 1999, Northwestern University: U. S.#5,744, 777 and 5,858,470.
14. W. J. PARKER, R. J. JENKINS, C. P. BUTLER and G. L. ABBOTT, *J. Appl. Phys.* **32**(9) (1961) 1679.
15. H. WANG, R. B. DINWIDDIE and P. S. GAAL, in "Thermal Conductivity 23," edited by R. B. Dinwiddie, K. E. Wilkes and R. S. Graves (Technomic Publishing, Lancaster, 1996) p. 119.
16. ASTM-E1461, (1992) 933.
17. L. M. CLARK III and R. E. TAYLOR, *J. Appl. Phys.* **46**(2) (1975) 714.
18. K. D. SHEFFLER and D. K. GUPTA, *J. Engr. Gas Turbine and Power* **110** (1988) 605.
19. K. MURALEEDHARAN, J. SUBRAHMANYAM and S. B. BHADURI, *J. Amer. Ceram. Soc.* **71**(5) (1988) C-266.
20. S. BOIRE-LAVIGNE, C. MOREAU and R. G. SAINT-JACQUES, *J. Thermal Spray Tech.* **4**(3) (1995) 261.
21. P. MORRELL and R. TAYLOR, *High Temperatures—High Pressures* **17** (1985) 79.
22. R. G. MUNRO, *J. Amer. Ceram. Soc.* **80**(8) (1997) 1919.
23. H. WANG and R. B. DINWIDDIE, *J. Thermal Spray Tech.* **9** (2000) 210.
24. D. P. H. HASSELMAN, L. F. JOHNSON, L. D. BENTSEN, R. SYED, H. L. LEE and M. V. SWAIN, *Am. Ceram. Soc. Bull.* **66**(5) (1987) 799.
25. G. E. YOUNGBLOOD, R. W. RICE and R. P. INGEL, *J. Amer. Ceram. Soc.* **71**(4) (1988) 255.
26. C. MOREAU, P. FARGIER-RICHARD, R. G. SAINT-JACQUES and P. CIELO, *Surf. Coat. Tech.* **61** (1993) 67.
27. H. WANG, unpublished work (1996).
28. MCPHERSON and SHAFER, *Thin Solid Films* **97** (1982) 201.
29. R. DUTTON, R. WHEELER, K. S. RAVICHANDRAN and K. AN, *J. Thermal Spray Tech.* **9** (2000) 204.
30. R. E. TAYLOR, *Materials Science & Engineering A: Structural Materials: Properties, Microstructure & Processing* **2** (1998) 160.
31. R. A. MILLER, J. L. SMIALEK and R. G. GARLICK, in "Advances in Ceramics: Science and Technology of Zirconia," edited by A. H. Heuer and L. W. Hobbs (Amer. Ceram. Soc., Columbus, 1981) p. 241.
32. R. MCPHERSON, *J. Mater. Sci* **8** (1973) 851.
33. *Idem.*, *ibid.* **15** (1980) 3141.
34. A. L. DRAGOO and J. J. DIAMOND, *J. Amer. Ceram. Soc.* **60** (1967) 568.

Received 4 April
and accepted 27 November 2000